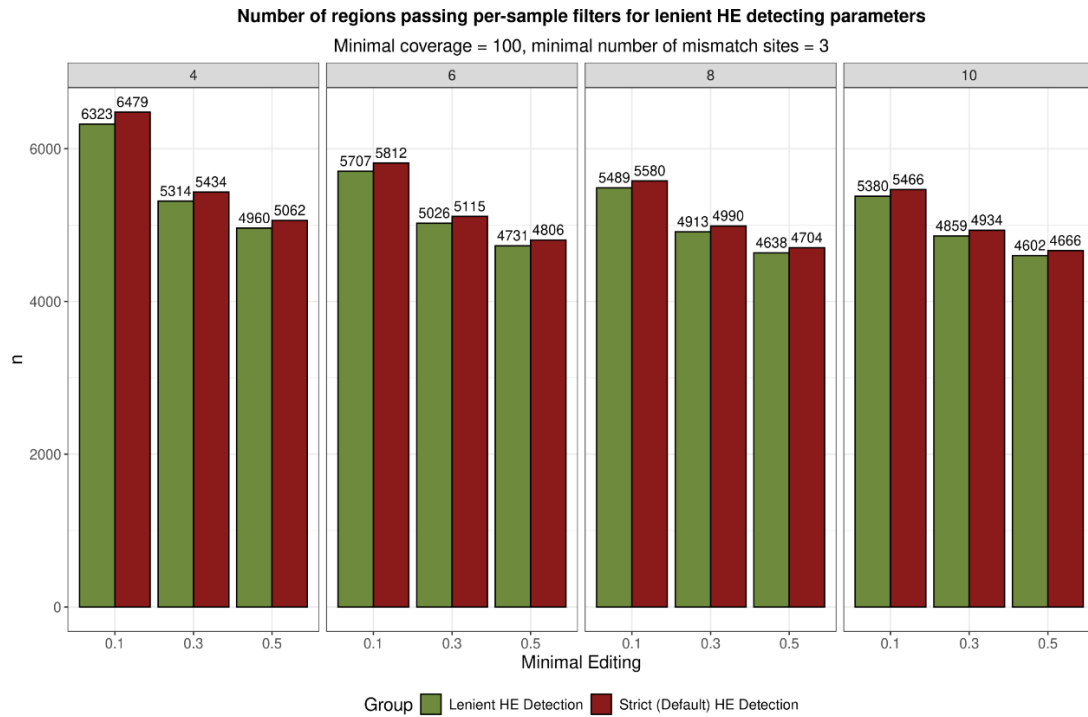
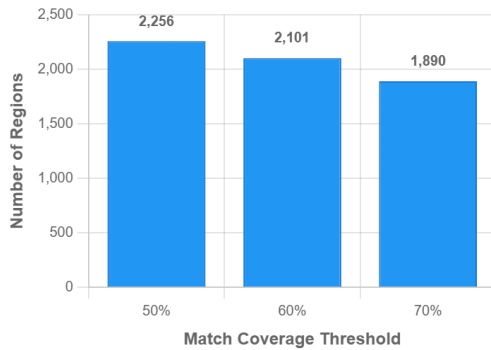


Figure S1: Number of hyper-edited region detected by mismatch type. Number of regions in which one finds hyper-editing on at least one strands, for each mismatch type (analysis of GTEx data).

A.



B. BLAST threshold sensitivity



C. RNAplfold threshold sensitivity

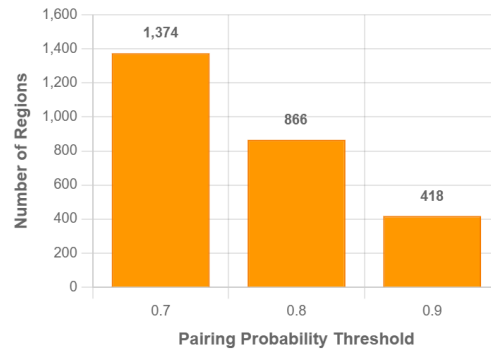


Figure S2: Sensitivity analyses for detection parameters and structural prediction thresholds. (A) Sensitivity analysis of hyper-editing detection parameters. Number of regions passing per-sample filters under different parameter combinations. Hyper-editing detection was performed using either strict (default: 5% mismatch density, 60% mismatch specificity) or lenient (4% mismatch density, 50% mismatch specificity) parameters. For each detection approach, regions were then filtered using varying signal-to-noise ratios (4, 6, 8, or 10-fold) and minimal editing thresholds (0.1%, 0.3%, or 0.5%). Green bars show lenient detection parameters; red bars show strict detection parameters. Numbers above bars indicate the count of regions passing all filters. Note that lenient hyper-editing parameters consistently yielded fewer final candidates because they initially detected more noisy regions with elevated non-A-to-G mismatches that were subsequently removed during quality filtering. (B) Number of regions with BLAST-detected intra-molecular complementary sequences under different match coverage thresholds. (C) Number of regions with RNAplfold-predicted secondary structures under different pairing probability thresholds.

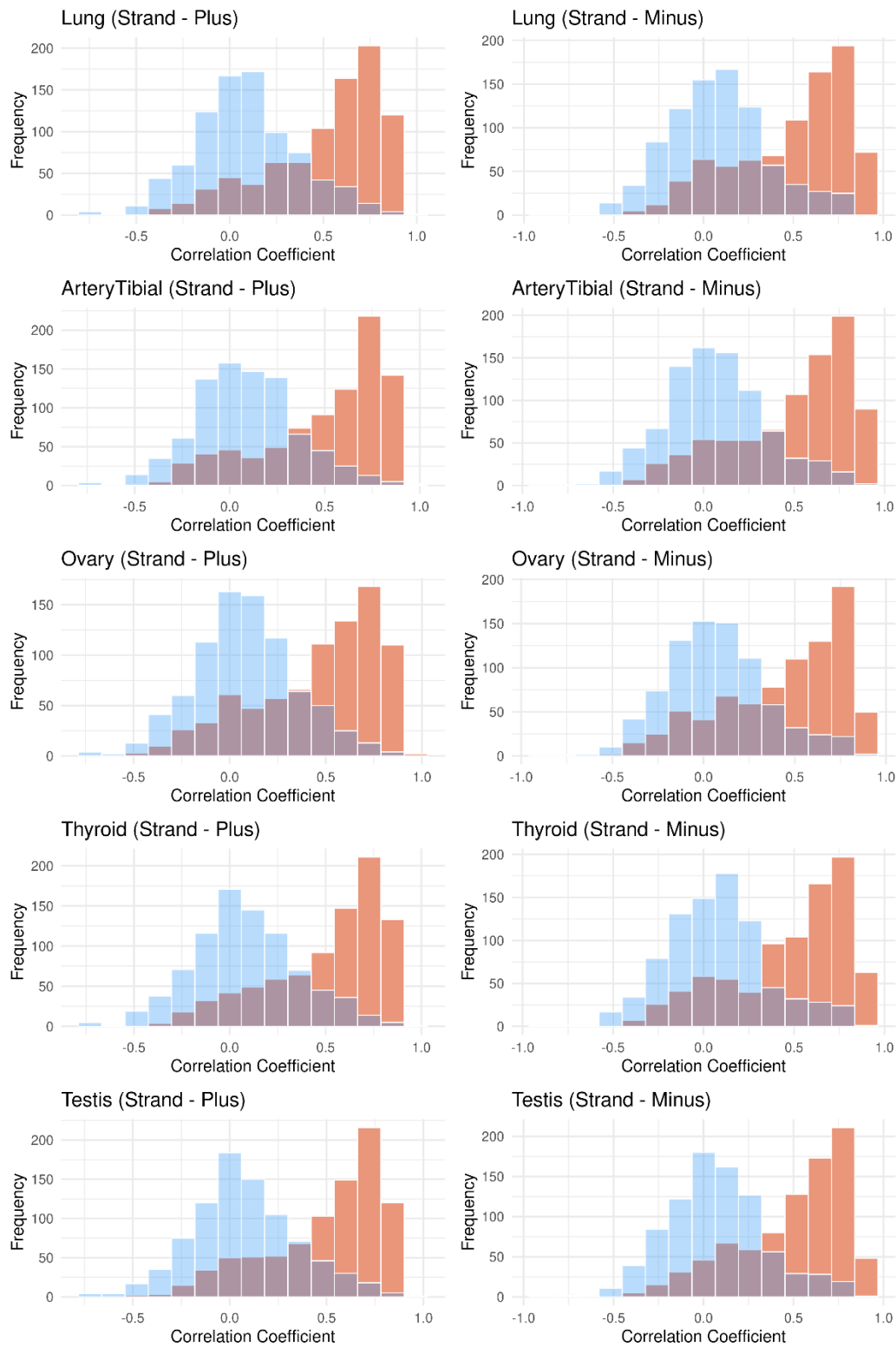


Figure S3: Distribution of correlation coefficients between editing indices and base-pairing probabilities across five tissues. For each tissue, the analysis is shown separately for the plus (left) and minus (right) strands. Regions with high pairing probability values (>0.8 , $n=866$) are marked in red, compared to the regions with the lowest base pairing probability ($n=866$; blue).

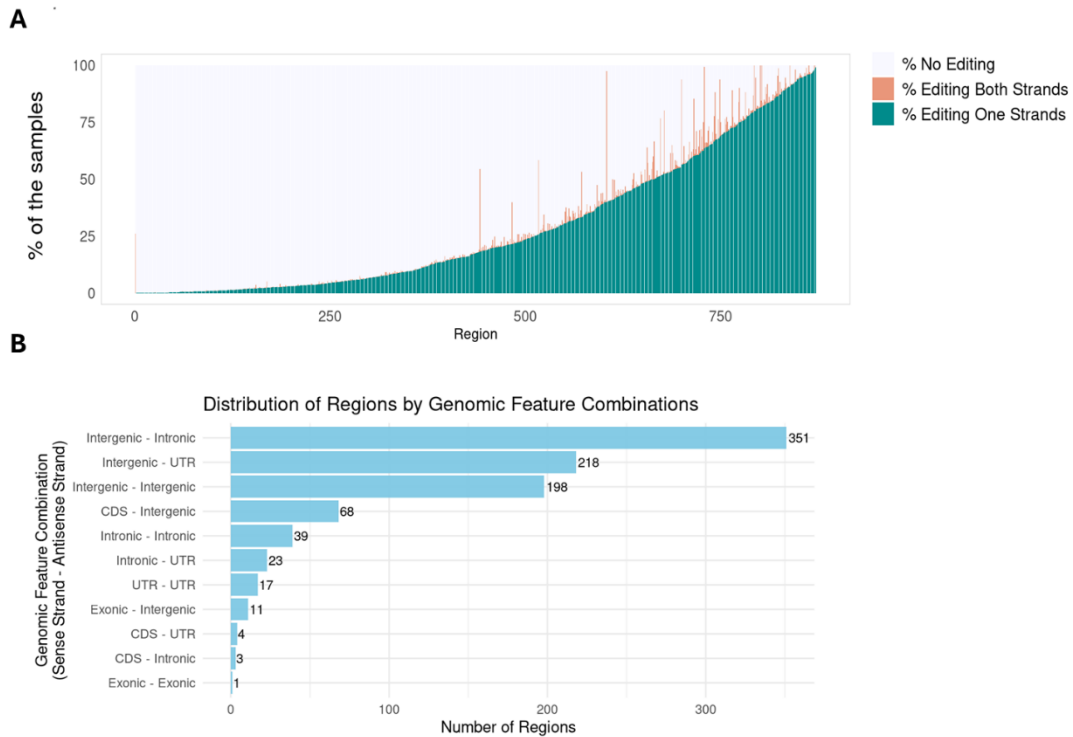


Figure S4: Analysis of regions lacking predicted secondary structures. (A) Samples exhibiting editing in the 872 regions lacking predicted secondary structures and passing editing detection criteria (≥ 5 samples with editing in at least one strand). Each row presents data for one candidate region, showing the percentage of samples in which editing is observed in both strands (pink) or only one strand (blue). Other samples have exhibited no detectable editing in the region. Data suggest that editing in these regions primarily occurs independently on individual strands, consistent with findings in regions with predicted secondary structures. (B) Detailed genomic feature combinations of the 933 regions without predicted intramolecular secondary structures. Categories represent sense strand genomic location followed by antisense strand genomic location. CDS = coding sequences; UTR = untranslated regions (3' and 5' combined); Exonic = other exonic regions. The analysis reveals that potential cis-NAT candidates are predominantly located in combinations involving intergenic and intronic regions, with coding sequences representing a small minority of cases.

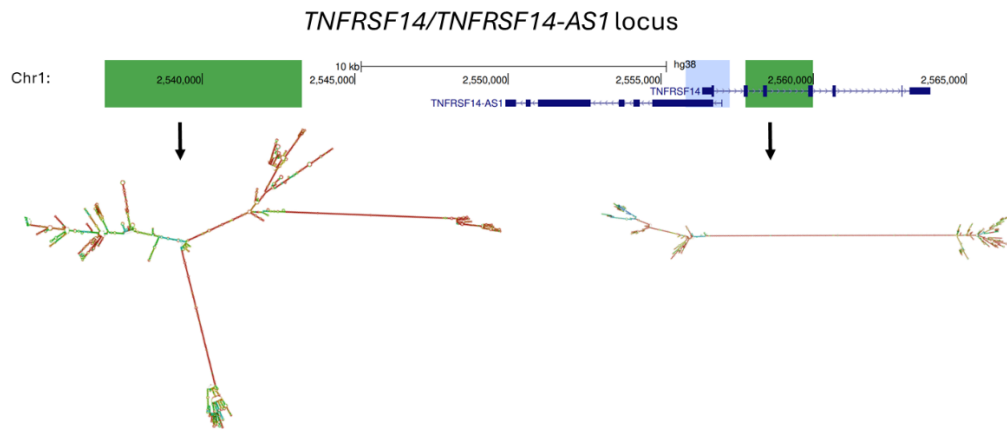


Figure S5: Analysis of the *TNFRSF14/TNFRSF14-AS1* locus. Genomic organization of Chr1:2534528-2565824 showing *TNFRSF14* and *TNFRSF14-AS1* transcripts. Green regions indicate areas where clusters of editing sites were detected. The blue region represents the direct overlap between sense and antisense transcripts where no significant editing was observed. Black arrows point to the editing clusters and their corresponding predicted intramolecular secondary structures (shown below).